

1 **"The final publication is available at [link.springer.com](https://link.springer.com)"**

2 **Effect of liquid impregnation on DBD atmospheric**  
3 **pressure plasma treatment of cotton**

4 Ricardo Molina<sup>a</sup>, Rim Bitar<sup>b</sup>, Pieter Cools<sup>b</sup>, Rino Morent<sup>b</sup>, Nathalie De Geyter<sup>b\*</sup>

5  
6 *<sup>a</sup>Department of Biological Chemistry, Plasma Chemistry Group, Institute of Advanced*  
7 *Chemistry of Catalonia (IQAC), Consejo Superior de Investigaciones Científicas (CSIC),*  
8 *Jordi Girona 18-26, 08034 Barcelona (Spain)*

9 *<sup>b</sup>Research Unit Plasma Technology (RUPT), Department of Applied Physics, Faculty of*  
10 *Engineering & Architecture, Ghent University (UGent), Sint-Pietersnieuwstraat 41, 9000*  
11 *Ghent, Belgium*

12 \*corresponding author: [Nathalie.DeGeyter@UGent.be](mailto:Nathalie.DeGeyter@UGent.be)

13

14 Acknowledgements

15 This work received financial support from the MAT2016-79866-R project (AEI/FEDER, UE). P. Cools would  
16 like to acknowledge the Special Research Fund of Ghent University for funding his post-doctoral mandate  
17 (BOF17/PDO/023). The authors would also like to thank the contribution of the scanning electron microscopy  
18 service of the Institute of Marine Sciences (ICM-CSIC).

19

20 Abstract

21 This paper describes the He non-thermal plasma treatment of liquid impregnated cotton fabrics. The cotton  
22 fabrics were soaked in either H<sub>2</sub>O, D<sub>2</sub>O or ethanol after which they were placed in an atmospheric pressure  
23 parallel-plate DBD reactor. The influence of the used liquid in combination with the plasma exposure time was  
24 studied using OES, FTIR, XPS and SEM. The addition of (deuterated) water was found to aid more efficiently in  
25 the incorporation of polar functional groups onto the cotton surface in comparison to a pure He plasma treatment.  
26 The presence of H and OH species in the discharge also caused extensive etching of the surface, which led to the  
27 formation of microcraters. The impregnation with ethanol was responsible for the formation of a plasma-based  
28 thin film on top of the cotton substrate, which was characterized by a high content of C-C bonds and a smooth  
29 surface morphology. These results show that the soaking of cotton fabric prior to plasma exposure can help to  
30 more effectively alter its surface properties compared to a dry plasma treatment.

31

32 **Keywords:** Cotton, DBD, Impregnation, Plasma treatment

33 **Introduction**

34 Non-thermal plasma treatments using oxygen-rich discharge gases are known to introduce a  
35 variety of polar oxygen-containing functional groups onto the surface of cellulosic materials  
36 including -OH, C=O and O-C=O groups, which can greatly enhance the surface wettability,  
37 dyeability and adhesion of biopolymer coatings such as chitosan. Several papers have already  
38 investigated the effect of atmospheric pressure non-thermal (or cold) plasma treatment on the  
39 properties of cotton fabrics (Aileni et al. 2019; Haji 2017; Haji 2019; Haji et al. 2013; Haji et

40 al. 2016; Patino et al. 2011; Rajasekaran and Muthuraman 2019; Sun and Stylios 2004; Wang  
41 et al. 2019). In particular, non-thermal plasma activation in the presence of water in liquid or  
42 vapor phase is a well-known technique to incorporate functional groups onto a polymer  
43 surface. In this context, underwater plasma treatments have been studied sporadically to  
44 fabricate substrates with homogeneous monofunctional surfaces (Joshi et al. 2009b), to induce  
45 direct functionalization, stimulate cross-linked layer formation and/or to graft or deposit  
46 mono-functional layers (Friedrich et al. 2008; Joshi et al. 2013; Joshi et al. 2009a; Joshi et al.  
47 2008; Khlyustova et al. 2015). Despite these promising results, the presence of moisture  
48 during a plasma surface treatment is often still viewed upon as an impurity (Ananth and Mark  
49 2008). As a result, to date, only few studies have looked at the intentional addition of  
50 liquids/vapors to discharge systems used for surface modification (Acseente et al. 2016; De  
51 Geyter et al. 2013; Van Deynse et al. 2014; Van Deynse et al. 2017). Moreover, most of these  
52 studies only focused on the addition of low amounts of vaporized water to the discharge gas  
53 (Acseente et al. 2016; De Geyter et al. 2013; Van Deynse et al. 2014). However, more recent  
54 studies have shown that, upon the addition of a liquid or vapor to the plasma discharge, the  
55 steady-state wettability of the plasma-exposed surface can be effectively altered, opening up  
56 new possibilities for enhanced surface modification of different substrates (Acseente et al.  
57 2016; De Geyter et al. 2013; Van Deynse et al. 2014; Van Deynse et al. 2017). Within our  
58 research facilities, research in recent years has been focused on the impregnation of porous  
59 polymeric materials (e.g. cotton, filter paper) with precursor solutions to obtain polymer-like  
60 coatings by means of *in-situ* plasma polymerization (Molina et al. 2014; Molina et al. 2017b).  
61 Whereas for plasma polymerization where precursors are applied in the gas phase, the coating  
62 properties are modulated by the precursor flow rate, system pressure, discharge power and  
63 plasma treatment time (Yasuda and Hirotsu 1978), plasma polymerization ignited onto a  
64 liquid-impregnated substrate is usually modulated by tuning the concentration of the precursor  
65 present in the liquid (Molina et al. 2014). However, to the best of our knowledge, the direct  
66 functionalization of a porous polymeric substrate by non-polymerizable liquid impregnation  
67 plasma has not been studied in detail until now. For this reason, in this study, cotton fabrics  
68 were therefore impregnated in either H<sub>2</sub>O, D<sub>2</sub>O or ethanol (EtOH) prior to performing plasma  
69 surface treatments. Helium (He) was chosen as discharge gas since a global model of He/H<sub>2</sub>O  
70 plasma chemistry in a parallel plate DBD reported the abundance of H<sub>2</sub>O<sup>+</sup>, water cluster ions,  
71 atomic and molecular metastable oxygen, OH(A) metastables and different ground-state  
72 neutrals such as H, O, H<sub>2</sub>, O<sub>2</sub>, OH, HO<sub>2</sub> and H<sub>2</sub>O<sub>2</sub> in He/H<sub>2</sub>O plasmas, with varying densities  
73 depending on the concentration of water vapor in the feeding gas (Liu et al. 2010). By first  
74 impregnating the cotton samples in water, the hypothesis is that the local concentration of  
75 water molecules at the substrate-plasma interface can be greatly enhanced, which may have a  
76 positive effect on the plasma surface modification process. Moreover, by replacing normal  
77 water with its deuterated form, better insights can be acquired on the role that H and OH  
78 species play in the surface modification processes. Finally, impregnation with EtOH is also  
79 examined as it can also introduce additional OH species in the plasma, which may in turn  
80 enhance the plasma surface treatment effects. Analysis of the active plasma species present in  
81 the plasma gas phase was done by optical emission spectroscopy (OES), while the plasma-  
82 induced effects on the cotton fabrics were analyzed by X-ray photoelectron spectroscopy  
83 (XPS), Fourier-transform infrared spectroscopy (FTIR) and scanning electron microscopy  
84 (SEM).

85

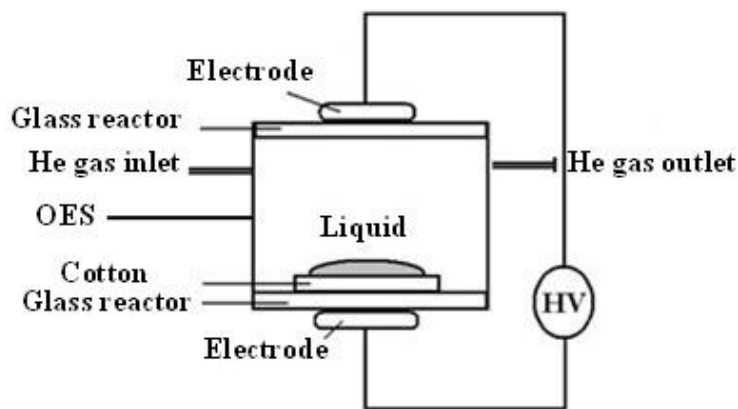
## 86 **Experimental**

87 **Materials**

88 Cotton fabrics (plain weave, woven textiles, bleached without optical brightener with a 180  
89 g/m<sup>2</sup> weight, article 210 from EMPA) were used as substrates. Concentrated detergent for pre-  
90 treating textiles (Tanaterge® Advanced) was acquired from Tanatex. Cotton was first  
91 conditioned by washing the fabric for 45 minutes at 60°C, under constant stirring at 250 rpm.  
92 The washing solution was prepared using Tanaterge® as detergent at 2 g/L concentration and  
93 washing was carried out at a 1/25 (w/v) load/wash solution ratio. Subsequently, the fabric was  
94 rinsed by placing it into deionized water for 20 minutes. Finally, the cotton fabric was dried  
95 and stored in a conditioned room at 67% relative humidity (RH) at a temperature of 24°C.  
96 Deionized water, deuterium oxide (D<sub>2</sub>O) with D<sub>2</sub> ≥ 99.96% provided by Eurosi-top and EtOH  
97 of absolute degree provided by Merck were used as impregnation liquids.  
98

99 **Impregnation and plasma treatment**

100 A DBD reactor operating at atmospheric pressure was used in this work, similar to the one  
101 reported in previous work (Jovančić et al. 2016; Molina et al. 2013a) and is schematically  
102 depicted in Figure 1. A gas mass flow controller (Bronkhorst, the Netherlands) was used to  
103 introduce helium gas at a fixed rate of 5 standard liters per minute (5 slm) in the reactor  
104 chamber between the upper and lower electrode, which were both covered with a dielectric  
105 material (borosilicate glass). The gas gap between the two dielectrics was maintained at 12  
106 mm and the volume between the electrodes was approximately ~0.1 liters. A 16-kHz AC  
107 signal was generated with a GF-855 function generator (Promax, Spain) connected to a linear  
108 amplifier AG-1012 (T&C Power Conversion, USA). A matching network and two  
109 transformers (HR-Diemen S.A., Spain) were also connected to the amplifier output to increase  
110 the output voltage up to approximately 20 kV peak-to-peak. The incident power in the plasma  
111 reactor was kept constant at 30 W.  
112



113

114 **Fig.1** Experimental atmospheric plasma set-up scheme

115 Cotton fabrics (3 x 3 cm<sup>2</sup>, ~0.16 gr) were introduced into the plasma reactor by placing these  
116 on the lower dielectric plate and 100 µl of the impregnation liquid (H<sub>2</sub>O, D<sub>2</sub>O or EtOH) was  
117 placed onto the cotton substrates (see Figure 1). The liquid weight with respect to the weight

118 of the cotton samples used in the experiments is equal to 0.5-0.7 gr liquid/1 gr cotton. Since  
119 the water absorption capacity of bleached cotton is ~2 gr water/1 gr cotton, plasma treatment  
120 was performed immediately after liquid impregnation in order to form a thin film of liquid on  
121 the cotton substrates before equilibrium of the liquid absorption capacity is reached (Hsieh et  
122 al. 1996). Subsequently, a plasma treatment in helium was carried out for a fixed period of  
123 300 s. A control sample was also prepared by performing the helium plasma treatment step on  
124 a cotton sample without any impregnation. In addition, a single cycle of consecutive cotton  
125 impregnation and posterior He plasma treatment (300 s) was also repeated 3 and 6 times.  
126

## 127 **OES analysis**

128 OES analysis was used to characterize the plasma active species inside the He discharge  
129 during surface modification. Diagnostics of the plasma gas was carried out with a quartz optic  
130 fiber connected to a Black Comet spectrometer (Stellarnet, USA) with concave gratings.  
131 Spectra were recorded in the UV–VIS wavelength range 190–850 nm (spectral resolution of  
132 0.5 nm) with an integration time of 4 s and a solid angle of ~0.9 steradians. No UV emission  
133 was measured below ~280 nm, since the DBD plasma reactor is made of borosilicate glass.  
134 The exact location of the quartz optic fiber in the DBD reactor can be seen in Figure 1.  
135

## 136 **Attenuated Total Reflectance FTIR (ATR-FTIR) measurements**

137 ATR-FTIR spectra of untreated and plasma-modified cotton fabrics were collected using a  
138 Nicolet Avatar 360 spectrometer equipped with a Smart iTR ATR sampling accessory  
139 (Thermo Scientific, USA). Spectra were obtained with an average of 32 scans using a  
140 resolution of 4 cm<sup>-1</sup>. An advanced ATR correction algorithm (OMNIC 7.3 from Thermo  
141 Electron Corporation) was used to correct for band intensity distortion, peaks shifts and  
142 polarization effects. Corrected ATR-FTIR spectra were found highly comparable to their  
143 transmission equivalents (Molina et al. 2013b). The background signal was extracted by  
144 means of linear backgrounds performed between 4000-3665 cm<sup>-1</sup>, 3665-2987 cm<sup>-1</sup>, 2987-2634  
145 cm<sup>-1</sup>, 2634-1800 cm<sup>-1</sup>, 1800-1492 cm<sup>-1</sup>, 1492-1186 cm<sup>-1</sup> and 1186-830 cm<sup>-1</sup>. Spectra were  
146 normalized to the C-O stretching vibration peak of cellulose located at 1031 cm<sup>-1</sup>.  
147

## 148 **XPS analysis**

149 The surface chemical composition of the untreated and plasma-modified cotton fabrics was  
150 analyzed using a PHI 5000 Versaprobe II XPS device equipped with an Al K<sub>α</sub> X-ray source  
151 (hν = 1486.6 eV) operated at 25 W. XPS analysis was conducted on samples, which have  
152 been placed in the XPS introduction machine, within 1 month after plasma modification. All  
153 measurements were conducted in a vacuum of at least 10<sup>-6</sup> Pa and the photoelectrons were  
154 detected with a hemispherical analyzer positioned at an angle of 45° with respect to the  
155 normal of the sample surface. Survey scans and individual high resolution C1s spectra were  
156 recorded with a pass energy of 187.85 eV (eV step = 0.8 eV) and 23.5 eV (eV step = 0.1 eV)  
157 respectively. Binding energies were referenced to the C1s photoelectron peak position for C-  
158 O species at 286.5 eV (Molina et al. 2017a) or C–C species at 285.0 eV in case of the EtOH  
159 impregnated sample (Gorjanc et al. 2010). Surface elemental composition was determined  
160 after a linear background subtraction from the area of the different photoemission peaks using  
161 the corresponding sensitivity factors of the XPS machine (Castle 1984). In this paper, the

162 presented XPS results are the average of 3 different measurement points on a single cotton  
163 sample.

164

165

166

## 167 **SEM imaging**

168 Possible plasma-induced changes in the surface morphology of the cotton samples were  
169 recorded using a Hitachi S-3500N SEM device operated at 5 kV. Prior to SEM imaging, a  
170 Quorum Q150RS gold sputter coater was used to deposit a gold coating of a thickness of  
171 approximately 20 nm on the samples to minimize charging.

172

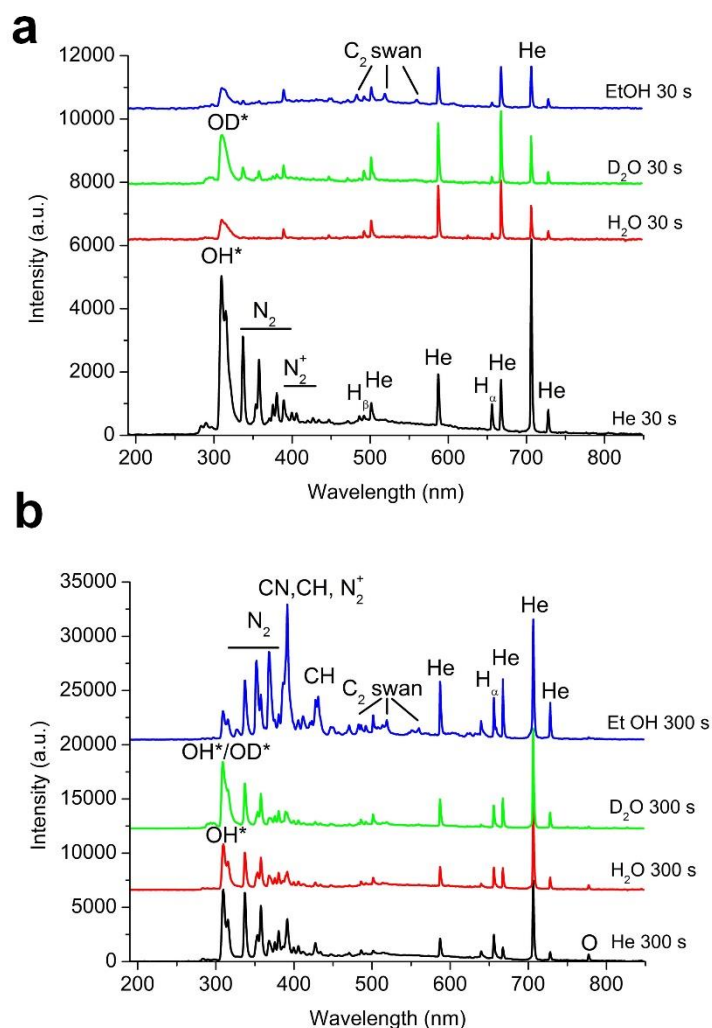
## 173 **Results**

174

### 175 **OES**

176 OES is a very powerful method to identify active species present in a plasma. The  
177 identification of said species is of great relevance in this work, as it can provide further  
178 insights into the occurring plasma/surface reactions. The UV-VIS emission spectra obtained  
179 during the He plasma treatment of cotton and cotton impregnated with different liquids  
180 (water, D<sub>2</sub>O and EtOH) are presented in Figure 2. The emission spectra recorded during the  
181 He plasma treatment of the non-impregnated cotton sample (Figure 2a and 2b) present  
182 different emission lines characteristic for atomic He (501.5 nm, 587.5 nm, 667.8 nm, 706.5  
183 nm, 728.1 nm). In addition, emission bands due to N<sub>2</sub><sup>+</sup> (391.4 nm, 427.8 nm, 470 nm), N<sub>2</sub>  
184 (315.9 nm, 337.1 nm, 357.6 nm, 380.4 nm), OH radicals (OH<sup>\*</sup>: 308.9 nm, 287 nm) and  
185 emission lines due to H atoms (H<sub>α</sub> line at 656.3 nm and H<sub>β</sub> line at 486.1 nm) can also be  
186 observed in the OES spectra. The presence of these species can be mainly attributed to  
187 residual humid air remaining in the plasma reactor. The observed plasma species are in  
188 excellent agreement with earlier published OES results of helium discharges operating at  
189 atmospheric pressure (Asandulesa et al. 2010; Bierstedt et al. 2015). It is also important to  
190 mention that during He plasma treatment of the non-impregnated cotton sample the plasma is  
191 operating in a diffuse regime independent of the used plasma treatment time.

192



193

194 **Fig.2** UV-VIS emission spectra obtained during the He plasma treatment of cotton and cotton impregnated with  
 195 different liquids (H<sub>2</sub>O, D<sub>2</sub>O and EtOH) at 30 (a) and 300 s (b)

196

197 Figure 2 does however reveals small differences in the OES spectra as a function of plasma  
 198 treatment time for the He plasma treatment: at long plasma treatment time (300 s), an  
 199 emission line due to atomic oxygen (777.4 nm) appears which might suggest that possible  
 200 water evaporation from the non-impregnated cotton substrates occurs at longer plasma  
 201 treatment times. At the short plasma treatment time (30 s), the emission spectrum during the  
 202 He plasma treatment of cotton impregnated with water is mainly composed of emission  
 203 lines/bands corresponding to He, H and OH\*, the latter 2 mainly originating from the  
 204 dissociation of H<sub>2</sub>O used for the impregnation of the cotton samples. Furthermore, in contrast  
 205 to the OES spectrum obtained during the plasma treatment of pure cotton, only a single, very  
 206 small band attributed to N<sub>2</sub><sup>+</sup> species could be distinguished. However, at long plasma  
 207 treatment times (300 s) (Figure 2b), the emission spectrum during the He plasma treatment of  
 208 cotton impregnated with water again resembles that of pure He, indicating that within 300 s,  
 209 most of the impregnated water had been evaporated from the cotton substrate.

210 Emission spectra recorded during the plasma treatment of cotton impregnated with D<sub>2</sub>O  
211 resemble these of cotton impregnated with H<sub>2</sub>O. Emission bands due to N<sub>2</sub> and N<sub>2</sub><sup>+</sup> species  
212 are however more pronounced in case of the D<sub>2</sub>O impregnated sample when compared to the  
213 H<sub>2</sub>O impregnated cotton. In addition, a small additional OD<sup>\*</sup> emission band at 287 nm could  
214 also be observed resulting from the dissociation of D<sub>2</sub>O used to impregnate the cotton sample.  
215 It is also important to mention that when cotton is impregnated with H<sub>2</sub>O or D<sub>2</sub>O, two  
216 different plasma regimes can be observed as a function of plasma treatment time which can be  
217 clearly differentiated in the OES spectra by examining the intensity of the He line at 706.5  
218 nm. As the presence of filaments decreases the overall plasma light emission and thus also the  
219 intensity of the He line at 706.5 nm compared to the diffuse plasma regime, the following can  
220 be concluded: at short treatment times (30 s) in case of the H<sub>2</sub>O and D<sub>2</sub>O impregnated  
221 samples, the plasma is operating in the filamentary regime due to the presence of high  
222 amounts of H<sub>2</sub>O or D<sub>2</sub>O. In contrast, at longer treatment times (300 s), most of the liquids are  
223 evaporated and the plasma again operates in the diffuse mode similar as in case of the He  
224 treatment of the non-impregnated sample.

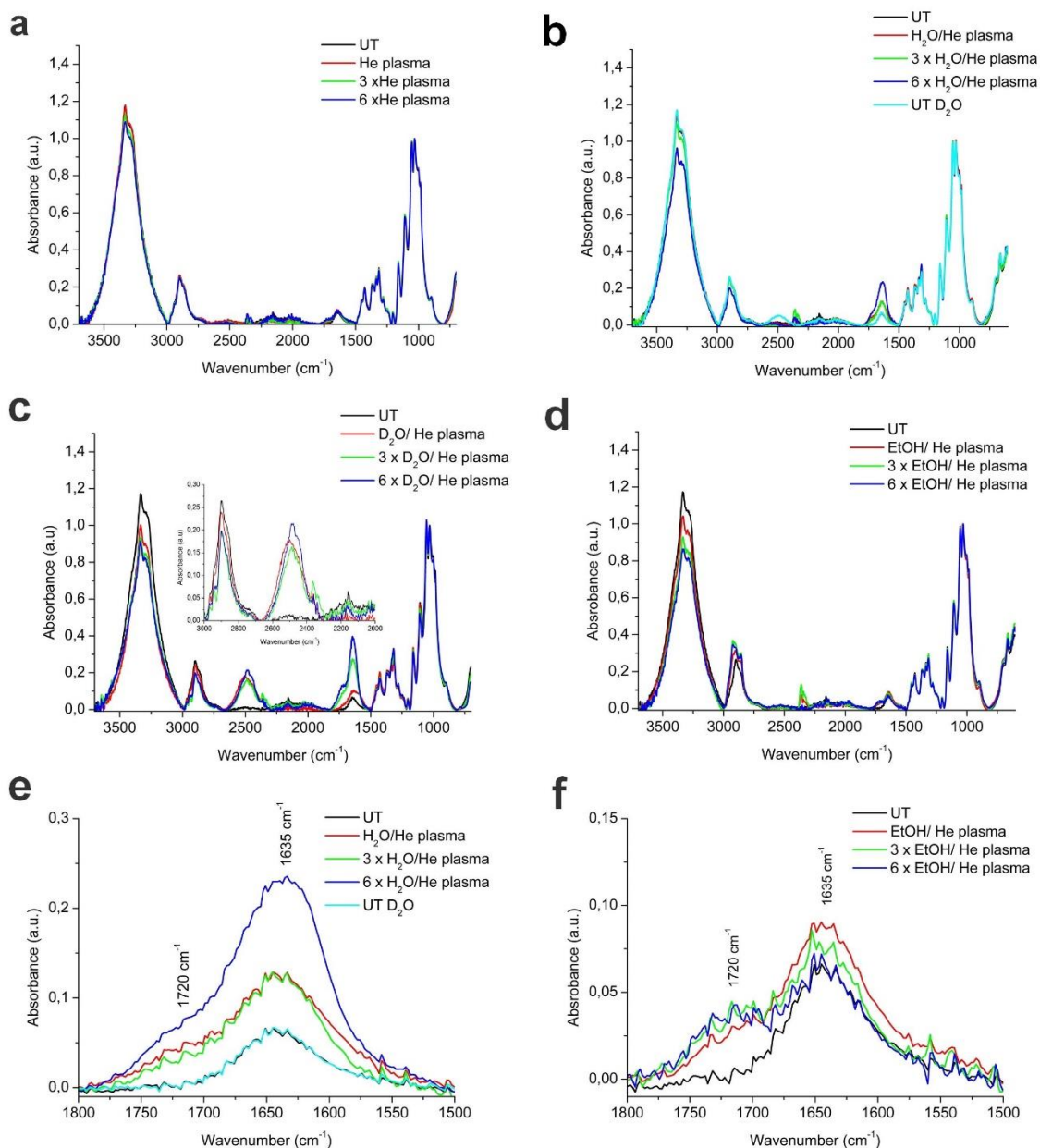
225  
226 During the He plasma treatment of cotton impregnated with EtOH, new emission bands  
227 attributed to carbon species (CN, CH and C<sub>2</sub>) could be observed at short plasma treatment  
228 times (30 s). These emission bands correspond to the CN violet system (360–390 nm), CH  
229 (430, 390 and 314 nm) and the C<sub>2</sub> Swan system ( $a^3\Pi_u - d^3\Pi_g$ ) consisting of various vibrational  
230 transitions (450–470 nm ( $\Delta v = -1$ ), 480–520 nm ( $\Delta v = 0$ ) and 520–570 nm ( $\Delta v = 1$ )). This is in  
231 accordance with literature and could be attributed to the dissociation of EtOH used for  
232 impregnation (Ikegami et al. 2004). In case of EtOH impregnation, emission bands due to  
233 carbon and nitrogen species resulting from ethanol dissociation could still be clearly  
234 distinguished after 300 s, whereas the atomic oxygen line was no longer recorded. These  
235 results provide a strong indication that the ethanol reforming had not yet been completed after  
236 300 s (Yanguas-Gil et al. 2004).

237

## 238 **ATR-FTIR**

239 Besides investigating the plasma gas phase, the effects of impregnation with different liquids  
240 (H<sub>2</sub>O, D<sub>2</sub>O and EtOH) and posterior He plasma treatment (300 s) on the chemical  
241 composition of the cotton substrates were also investigated by means of ATR-FTIR.

242



244  
 245 **Fig.3** ATR-FTIR spectra obtained on non-impregnated (a) and H<sub>2</sub>O (b), D<sub>2</sub>O (c) and EtOH (d) impregnated  
 246 cotton samples after 1, 3 and 6 cycles of consecutive impregnation/300 s He plasma treatment. UT stands for the  
 247 untreated cotton sample. Enlarged carboxylate region (1800-1500 cm<sup>-1</sup>) obtained for cotton samples impregnated  
 248 with H<sub>2</sub>O (e) and EtOH (f)

249  
 250 First of all, the ATR-FTIR spectra of untreated and He plasma-treated cotton samples are  
 251 presented in Figure 3A. The FTIR spectrum of untreated cotton shows multiple bands  
 252 characteristic for cellulose (Chung et al. 2004; Garside and Wyeth 2003): a very broad OH  
 253 stretching peak in the region 3750–2995 cm<sup>-1</sup>, a broad peak in the region 3000-2800 cm<sup>-1</sup>  
 254 attributed to CH stretching vibrations, a smaller but rather broad peak at ≈1635 cm<sup>-1</sup> which is  
 255 usually assigned to the OH bending mode of adsorbed water, a peak at 1430 cm<sup>-1</sup> due to CH  
 256 and C-OH bending vibrations, a broad peak in the region 1400-1300 cm<sup>-1</sup> due to CH and CH<sub>2</sub>  
 257 bending vibrations, a peak in the region 1160-1108 cm<sup>-1</sup> due to C-O-C stretching and a peak  
 258 in the region 1030-998 cm<sup>-1</sup> due to C-O stretching vibrations. Figure 3A reveals no significant



259 differences in the ATR-FTIR spectra of non-impregnated cotton samples after performing  
260 multiple consecutive He plasma treatments. This is in excellent agreement with earlier  
261 published results showing no differences in ATR-FTIR spectra of polymer films as a result of  
262 plasma surface treatment (Morent et al. 2008). Indeed, as plasma active species are only able  
263 to interact with the top few nanometers of a material, the penetration depth of ATR-FTIR is  
264 too large to detect the surface chemical changes induced by plasma treatment (Morent et al.  
265 2008).

266  
267 The ATR-FTIR spectra of cotton samples undergoing consecutive water impregnation and He  
268 plasma treatments are shown in Figure 3B. In contrast to the non-impregnated cotton sample,  
269 differences in ATR-FTIR spectra could be observed between the untreated and plasma-  
270 modified samples: with an increasing number of impregnation/plasma treatment cycles, the  
271 broad peak at  $1635\text{ cm}^{-1}$  gradually increases. A more detailed investigation of this  
272 wavenumber region (see Figure 3E) indicates that a new band attributed to carboxylate ( $\text{O}-$   
273  $\text{C}=\text{O}^-$ ) stretching vibrations appears at  $1720\text{ cm}^{-1}$  which gains in intensity as a function of  
274 treatment cycles. In addition, figure 3E also reveals that the peak at  $1635\text{ cm}^{-1}$  also increases  
275 as a function of impregnation/plasma treatment cycles. As the broad OH band in the region  
276  $3750\text{-}2295\text{ cm}^{-1}$  decreases with plasma treatment cycles, this increase at  $1635\text{ cm}^{-1}$  could thus  
277 not be attributed to higher amounts of adsorbed water, but is most likely the result of the  
278 generation of carbonyl groups ( $\text{C}=\text{O}$ ) as a consequence of the plasma-induced cotton  
279 oxidation process. This seems to be corroborated by the ATR-FTIR spectrum corresponding  
280 to untreated cotton immersed in  $\text{D}_2\text{O}$  for 24 hours and dried at room temperature (sample UT  
281  $\text{D}_2\text{O}$ ). The UT  $\text{D}_2\text{O}$  ATR-FTIR spectrum highly resembles the ATR-FTIR spectrum of  
282 untreated cotton (see Figure 3B and E), but a new band in the region  $2650\text{-}2250\text{ cm}^{-1}$   
283 associated to the OD stretching peak of  $\text{D}_2\text{O}$  can be observed in the former sample (see Figure  
284 3B). It could therefore be concluded that the intensity of the peak at  $1635\text{ cm}^{-1}$  should not only  
285 be attributed to the OH bending mode of adsorbed water but the possible signal formation of  
286 carbonyl groups should also be taking into account. These carbonyl groups could be formed in  
287 the untreated cotton samples as a consequence of the bleaching process carried out to the  
288 cotton prior to its use in this work.

289  
290 Similar trends are observed when  $\text{D}_2\text{O}$  is used as impregnation liquid (Figure 3C). The ATR-  
291 FTIR spectra also show an increasing peak at  $1635\text{ cm}^{-1}$  and at  $1720\text{ cm}^{-1}$ , proving the  
292 formation of carbonyl and carboxylate groups on the plasma-modified cotton samples. Similar  
293 as for the water impregnated samples, both peaks also increase with increasing treatment  
294 cycles, suggesting a higher incorporation of carbonyl and carboxylate groups with increasing  
295 impregnation/plasma treatment cycles. However, because of the different position of the OH  
296 stretching peak of  $\text{H}_2\text{O}$  ( $3750\text{-}2995\text{ cm}^{-1}$ ) and the OD stretching peak of  $\text{D}_2\text{O}$  ( $2650\text{-}2250\text{ cm}^{-1}$ ),  
297 a new band corresponding to the adsorbed  $\text{D}_2\text{O}$  in the cotton substrate also appears.  
298 Additionally, the H-O-H bending band of water ( $1638\text{ cm}^{-1}$ ) also shifts towards lower  
299 wavenumbers for D-O-D ( $1205\text{ cm}^{-1}$ ) (Belhadj et al. 2015; Liu et al. 2016). Nonetheless, the  
300 intensity of this band is typically much lower compared to the OD stretching band, making it  
301 difficult to clearly differentiate the D-O-D peak in the presented ATR-FTIR spectra.  
302 Additionally, it also seems that there is a correlation between the decrease in the band  
303 associated to the OH stretching peak ( $3750\text{-}2995\text{ cm}^{-1}$ ) of cellulose and the increase in the  
304 carbonyl and carboxylate groups as a consequence of a plasma-induced oxidation process and  
305 an interchange of OH groups present in the cotton substrates with OD groups. Therefore,  
306 when replacing  $\text{H}_2\text{O}$  by  $\text{D}_2\text{O}$ , it is again suggested that the increased peak at  $1635\text{ cm}^{-1}$  cannot  
307 be attributed solely to adsorbed  $\text{D}_2\text{O}$  and should thus be partially attributed to carbonyl groups  
308 formed because of cellulose oxidation ( $\text{C}=\text{O}$ ). Comparing the ATR-FTIR spectra of He

309 plasma-treated cotton with and without liquid impregnation, it seems that the presence of H<sub>2</sub>O  
310 or D<sub>2</sub>O favors the oxidation of cellulose because of the diffusion and formation of oxygen and  
311 nitrogen reactive species (ROS, RNS) in the adsorbed liquids (H<sub>2</sub>O<sub>2</sub>, OH<sup>•</sup>, O<sub>2</sub><sup>•-</sup>, ONOO<sup>-</sup> and  
312 NO<sup>•</sup>) (Brisset and Pawlat 2016; Gorbanev et al. 2016; Ikawa et al. 2010; Tani et al. 2012).

313  
314 The ATR-FTIR spectra corresponding to consecutive ethanol (EtOH) impregnation and He  
315 plasma treatments of cotton substrates (up to 6 impregnation/plasma treatments) are depicted  
316 in Figure 3D. In this particular case, a small increase in absorbance of the region  
317 corresponding to CH stretching modes (3000-2800 cm<sup>-1</sup>) is observed as a function of  
318 impregnation/plasma treatment cycles, suggesting the incorporation of hydrocarbon groups,  
319 which is in agreement with the obtained OES spectra showing the presence of excited carbon  
320 species in the plasma. Additionally, an increase in the band at 1720 cm<sup>-1</sup> is observed whereas  
321 the band at 1635 cm<sup>-1</sup> only marginally increases (see Figure 3F), suggesting that also in this  
322 case, plasma-assisted oxidation processes occur resulting in the incorporation of mainly  
323 carboxylate groups.

324

## 325 XPS

326 Since the analysis depth of ATR-FTIR is typically between 600 and 1000 nm, crucial  
327 information is lost from the uppermost polymer layers, which is particularly important in case  
328 of plasma surface modification, as non-thermal plasmas are known to primarily influence the  
329 first 50 nm of a material (Holländer et al. 1999; Tatoulian et al. 1995; Wang et al. 2008). In  
330 contrast, XPS analyses only the first 3-10 nm of a material surface, making it a very suitable  
331 technique to track plasma-induced surface changes (Castle 1984; Cools et al. 2015).  
332 Therefore, the changes in the surface chemical composition of the cotton substrates have also  
333 been studied by XPS in this work.

334

335 The atomic surface chemical composition of the He plasma-treated cotton samples and the  
336 cotton samples first impregnated with different liquids (water, D<sub>2</sub>O and EtOH) prior to plasma  
337 modification are presented in Table 1. Consecutive liquid impregnation and He plasma  
338 treatment steps of cotton substrates did not significantly change the surface elemental  
339 composition and for this reason, only results of first impregnation and He plasma treatment  
340 were mentioned in table 1. This latter reveals that the He plasma treatment of cotton substrates  
341 does not significantly change the atomic surface chemical composition with respect to the  
342 untreated one. This result is quite surprising as plasma-induced surface oxidation was  
343 expected, since OH radicals and atomic oxygen were observed in the OES spectra during He  
344 plasma treatment (Figure 2). It is also important to mention that the obtained O/C ratio for the  
345 untreated cellulose sample is considerably lower than the expected O/C ratio for pure  
346 cellulose (O/C = 0.83), which can be attributed to surface non-cellulosic components, which  
347 naturally occur on cotton (Kolarova et al. 2013) and which have not been removed from the  
348 samples by the performed washing step. Table 1 also reveals that if the cotton sample was  
349 first impregnated with H<sub>2</sub>O, no significant difference in oxygen content could again be  
350 observed. On the other hand, a small increase in oxygen content was observable on the D<sub>2</sub>O  
351 impregnated sample. Moreover, when cotton was impregnated with EtOH, a strong increase  
352 in carbon content combined with a large decrease in oxygen content was observed, which was  
353 highly unexpected.

354 Table 1. Elemental composition (%) at the surface determined by XPS on cotton treated by He plasma and cotton  
355 impregnated with different liquids and subsequently treated by He plasma (300 s).

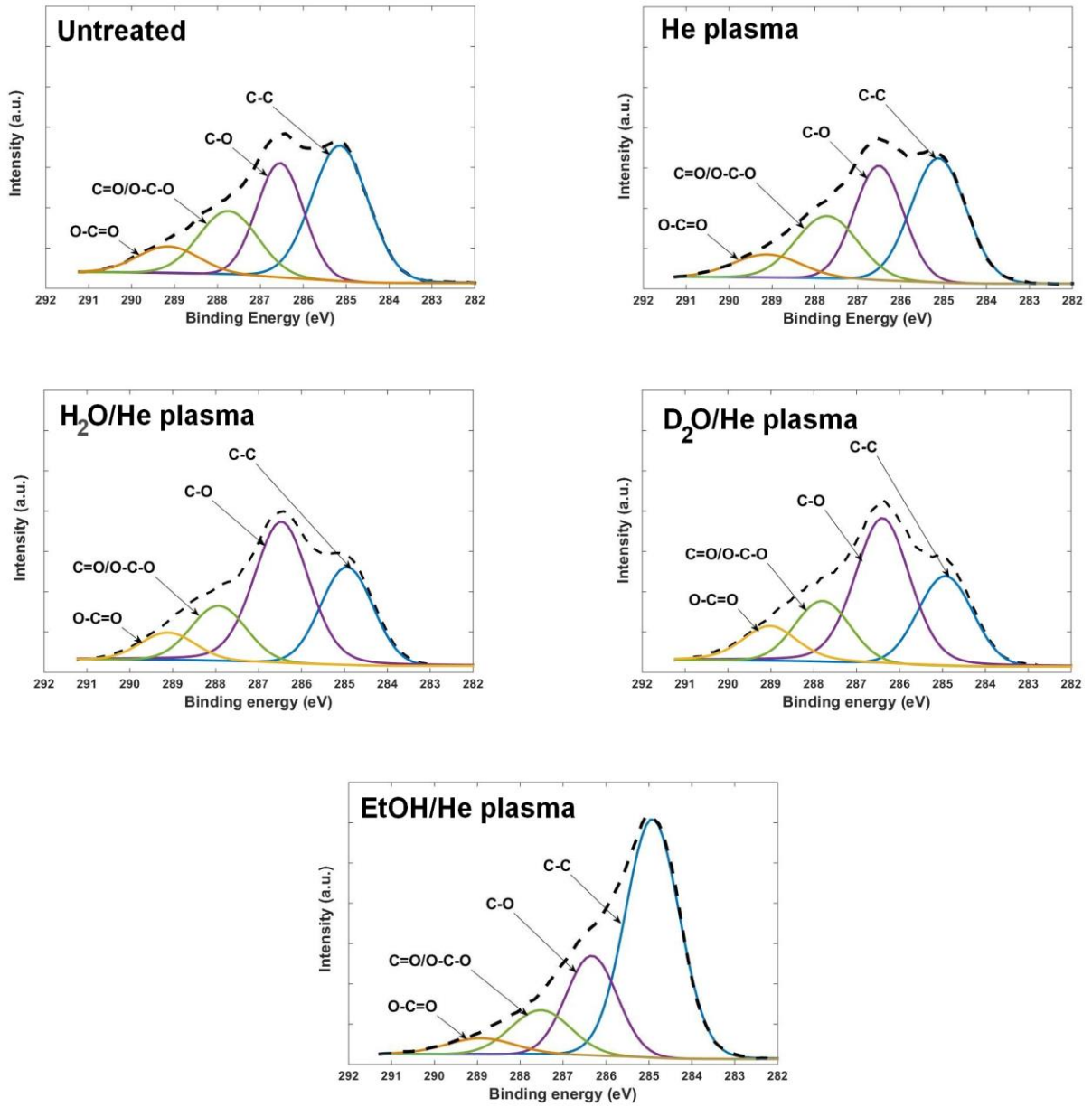
---

	C (%)	O (%)	O/C
Untreated	61.5±2.4	38.5±2.4	0.62
He plasma	61.8±1.8	38.2±1.8	0.61
H <sub>2</sub> O/He plasma	60.5±0.9	39.5±0.9	0.65
D <sub>2</sub> O/He plasma	57.8±0.9	42.2±0.9	0.72
EtOH/He plasma	85.9±1.2	14.1±1.2	0.16

---

356

357 High-resolution spectra of the C1s envelopes were also recorded to obtain additional insights  
358 into the chemical changes induced on the cotton substrates and the fitted C1s peaks are  
359 depicted in Figure 4 for a single cycle of impregnation and plasma treatment.



360

361 **Fig.4** XPS high-resolution C1s spectra of untreated cotton, cotton treated with He plasma and cotton  
 362 impregnated with different liquids and subsequently treated by He plasma

363 As shown in Figure 4, the C1s spectrum of the untreated cotton sample is deconvoluted into 4  
 364 distinct peaks, the largest peak being the one at  $286.5 \pm 0.1$  eV, corresponding to aliphatic C-  
 365 O-/C-OH functionalities, as expected for cellulose. Two shoulder bands at higher binding  
 366 energies are also observed that can be attributed to O-C-O/C=O functionalities ( $287.7 \pm 0.1$   
 367 eV), which are present in the chemical structure of cellulose and O-C=O functionalities ( $289.1$   
 368  $\pm 0.1$  eV) most likely originating from the bleaching process carried out on the cotton samples  
 369 (Molina et al. 2017a; Patino et al. 2011). Moreover, a peak at  $285.0 \pm 0.1$  eV needs to be  
 370 included as well to obtain a good fit of the C1s peak: this peak probably originates from some  
 371 non-cellulosic components such as waxes, proteins or pectin, which typically cover natural  
 372 cotton fibers (Topalovic et al. 2007). Figure 4 also reveals that after performing the different  
 373 plasma modification procedures, similar XPS fitting peaks as the ones used for the untreated  
 374 cotton sample can still be applied to deconvolute the high resolution C1s spectra of the  
 375 plasma-modified samples, although the area below each individual peak seems to vary  
 376 depending on the performed plasma modification step. From these fitted spectra, relative  
 377 concentrations of the different carbon bonds present at the surface of the cellulose samples  
 378 can be determined and these quantitative results are presented in Table 2 for all samples under  
 379 study using a single cycle of impregnation and plasma treatment.

380 Table 2. Relative concentrations of carbon bonds on untreated cotton, cotton treated with He plasma and cotton  
 381 impregnated with different liquids and subsequently treated by He plasma.

Sample	C-C	C-O-/ C-OH	C=O/ O-C-O	O-C=O
Untreated	$41.3 \pm 0.3$	$35.0 \pm 0.1$	$14.6 \pm 0.3$	$9.1 \pm 0.5$
1x He	$39.1 \pm 0.5$	$35.9 \pm 0.5$	$15.6 \pm 0.2$	$9.4 \pm 0.5$
1x H <sub>2</sub> O	$30.0 \pm 2.0$	$42.9 \pm 2.1$	$16.3 \pm 0.7$	$10.8 \pm 0.8$
1x D <sub>2</sub> O	$25.3 \pm 1.6$	$45.6 \pm 1.6$	$17.5 \pm 0.4$	$11.6 \pm 2.8$
1x EtOH	$60.4 \pm 2.6$	$23.6 \pm 0.5$	$11.6 \pm 1.9$	$4.4 \pm 1.0$

382

383 This table clearly reveals that the He plasma treated cotton has a surface chemical  
 384 composition which closely resembles the surface chemical composition of the untreated  
 385 cotton sample, which is consistent with the results shown in Table 1. As such, it can thus be  
 386 concluded that the performed helium plasma treatment does not induce a significant surface  
 387 oxidation, although reactive oxygen plasma species are present in the discharge. Most likely, a  
 388 combination of functionalization and etching simultaneously occurs leading to an unaffected  
 389 total oxygen content after He plasma treatment. Table 2 also shows that when performing the  
 390 plasma treatment on the H<sub>2</sub>O impregnated sample, a more pronounced increase in oxygen-  
 391 containing surface functional groups is obtained: a considerable increase in the amount of C-  
 392 O, C=O/O-C-O and O-C=O groups can be seen upon plasma treatment. This increase in C-O,  
 393 C=O/O-C-O and O-C=O groups is even more pronounced when the cotton sample is first

394 impregnated in D<sub>2</sub>O, which is in agreement with the O/C ratio results given in Table 1. The  
395 XPS results in this section thus confirm the incorporation of C=O and O-C=O groups on the  
396 cotton surface, which was also seen in the ATR-FTIR spectra shown in the previous section  
397 and additionally also reveal the incorporation of C-O functional groups on the cotton surface.  
398 Taking into account the considerably large penetration depth of FTIR ( $\approx 0.6-1 \mu\text{m}$ ), it can also  
399 be concluded that the C=O and O-C=O functional groups are not only incorporated at the  
400 surface of the cotton samples, but also in the subsurface region.

401  
402 When examining the samples impregnated with ethanol prior to plasma treatment, a  
403 completely different trend can be observed: a strong decrease in the oxygen-containing  
404 functional groups occurs in combination with a large increase in the amount of C-C groups.  
405 This peculiar result suggests the formation of a thin oxygenated hydrocarbon coating on the  
406 cotton sample, which will be further confirmed by SEM imaging performed in the following  
407 section.

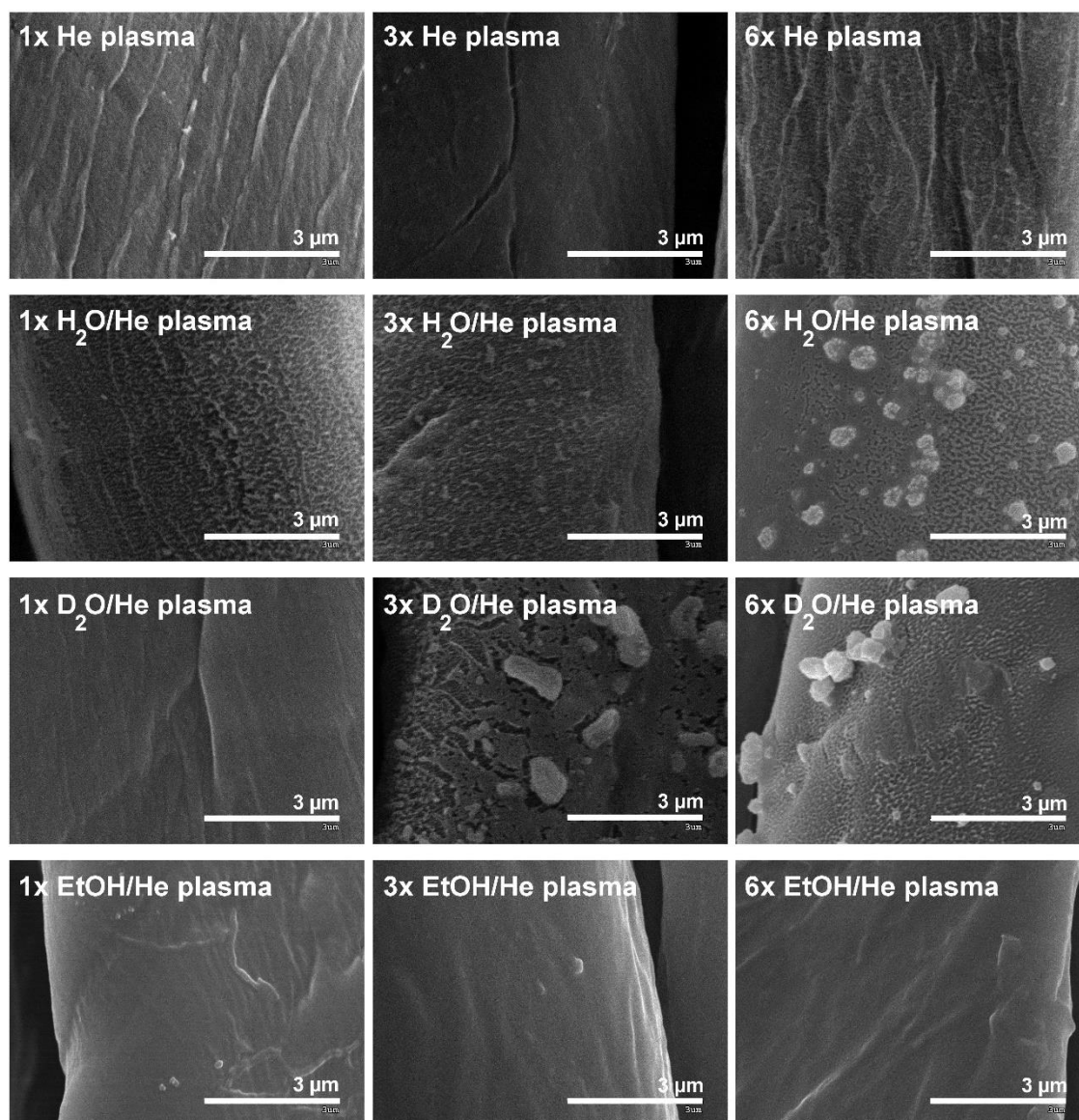
408

#### 409 **SEM**

410 Possible surface damage induced by the performed plasma treatments was also investigated  
411 by SEM and the obtained SEM images are shown in Figure 5.

412

413



414

415 **Fig.5** SEM images of cotton treated with He plasma and cotton impregnated with different liquids and  
 416 subsequently treated by He plasma

417

418 A single He plasma treatment is found to have a minimal impact on the surface morphology  
 419 of the cotton sample, as a similar physical appearance compared to the untreated cotton was  
 420 recorded (not shown for reader clarity). In contrast, a more profound impact on the surface  
 421 integrity is observed with increasing repetitions of He plasma treatments. After 6 He plasma  
 422 treatments, the cotton surface exhibits some surface damage in the form of microcraters due to  
 423 plasma-induced etching processes (Karahan and Özdoğan 2008). Similar morphological  
 424 changes have been reported when performing corona plasma treatments of cotton (Mihailović  
 425 et al. 2011).

426

427 On the other hand, when cotton is first impregnated either with H<sub>2</sub>O or D<sub>2</sub>O and subsequently  
 428 exposed to the He plasma, profound topographic changes could be observed even after one  
 429 treatment cycle. In addition, by increasing the number of impregnation/plasma treatments, the  
 430 observed surface damage significantly increases and after 6 impregnation/plasma treatment

431 cycles, structures similar to particles appear on the cotton fibers, proving the excessive  
432 damage to the cotton fibers because of the high plasma exposure times. It is suggested that the  
433 presence of H<sub>2</sub>O or D<sub>2</sub>O on the cotton surface may induce many streamers/filaments during  
434 plasma treatment which could in turn be responsible for the excessive damage promoted on  
435 the cotton surface when compared to the He treatment without impregnation. This hypothesis  
436 was further confirmed by the OES results, which revealed that the He plasma on the H<sub>2</sub>O and  
437 D<sub>2</sub>O impregnated cotton samples operated in the filamentary mode at treatment times below  
438 300 s.

439  
440 When EtOH is used as impregnation liquid prior to the He plasma treatment, it could be  
441 observed that the cotton surface is covered with a flat coating, which is in agreement with the  
442 conclusions drawn from XPS analysis. In the case of ethanol impregnation, a plasma  
443 deposition process thus takes place instead of a plasma activation process. The film-forming  
444 behavior of EtOH-enriched plasmas has already been described before (Van Deynse et al.  
445 2017), thereby further confirming the results obtained in this work. It is also important to  
446 mention that the presence of this film does not produce any significant visual color change of  
447 the cotton substrates.  
448

## 449 **Conclusions**

450 In this study, cotton fibers were impregnated with H<sub>2</sub>O, D<sub>2</sub>O or EtOH prior to an atmospheric  
451 pressure He plasma treatment in a parallel-plate DBD set-up. OES analysis showed an  
452 increase in H atoms and OH radicals during the plasma treatment of H<sub>2</sub>O impregnated cotton  
453 samples, as was to be expected. Replacing water with its deuterated counterpart resulted in  
454 higher concentrations of N metastable species, which showed the indirect influence of free H  
455 species in the plasma. Ethanol plasma induced the formation of a variety of CN, C and CO  
456 species, even after longer treatment times, indicating that the presence of carbon induced a  
457 completely different plasma chemistry. Chemical analysis of the cotton samples revealed that  
458 the impregnation with (deuterated) water resulted in a more efficient plasma-induced  
459 oxidation of the cotton compared to the dry plasma treatment, while the presence of ethanol  
460 led to the formation of a thin oxygenated hydrocarbon film on top of the cotton sample. SEM  
461 analysis showed the profound etching of the cotton fibers as a result of the presence of the  
462 (deuterated) water, while for the EtOH impregnated samples, a smooth morphology could be  
463 distinguished, further indicating the presence of the thin film. Overall, it can be concluded that  
464 the impregnation of cotton fabrics with a variety of liquids can induce a more efficient surface  
465 modification compared to a plasma treatment as such.

## 466 **References**

- 467 Acse T, Ionita MD, Teodorescu M, Marascu V, Dinescu G (2016) Surface modification of  
468 polymethylmethacrylate foils using an atmospheric pressure plasma jet in presence of water vapors.  
469 *Thin Solid Films* 614:25-30. <https://doi.org/10.1016/j.tsf.2015.12.037>
- 470 Aileni RM, Albici S, Chiriac L, Subtirica A, Dinca LC (2019) Aspects of the hydrophobic effect sustainability  
471 obtained in plasma for cotton fabrics. *Ind. Textila* 70:223-228. <http://doi.org/10.35530/IT.070.03.1475>
- 472 Ananth NB, Mark JK (2008) Repetitively pulsed atmospheric pressure discharge treatment of rough polymer  
473 surfaces: II. Treatment of micro-beads in He/NH<sub>3</sub>/H<sub>2</sub>O and He/O<sub>2</sub>/H<sub>2</sub>O mixtures. *Plasma Sources Sci.  
474 Technol.* 17:035025. <http://doi.org/10.1088/0963-0252/17/3/035025>



475 Asandulesa M, Topala I, Dumitrascu N (2010) Effect of helium DBD plasma treatment on the surface of wood  
476 samples. *Holzforschung* 64:223-227. <http://doi.org/10.1515/hf.2010.025>

477 Belhadj H, Hakki A, Robertson PK, Bahnemann DW (2015) In situ ATR-FTIR study of H<sub>2</sub>O and D<sub>2</sub>O  
478 adsorption on TiO<sub>2</sub> under UV irradiation. *Phys. Chem. Chem. Phys.* 17:22940-22946.  
479 <http://doi.org/10.1039/C5CP03947A>

480 Bierstedt A, Panne U, Rurack K, Riedel J (2015) Characterization of two modes in a dielectric barrier discharge  
481 probe by optical emission spectroscopy and time-of-flight mass spectrometry. *J Anal. At. Spectrom.*  
482 30:2496-2506. <http://doi.org/10.1039/c5ja00332f>

483 Brisset J-L, Pawlat J (2016) Chemical effects of air plasma species on aqueous solutes in direct and delayed  
484 exposure modes: discharge, post-discharge and plasma activated water. *Plasma Chem. Plasma Process.*  
485 36:355-381. <http://doi.org/10.1007/s11090-015-9653-6>

486 Castle JE (1984) Practical surface analysis by Auger and X-ray photoelectron spectroscopy. D. Briggs and M. P.  
487 Seah (Editors). John Wiley and Sons Ltd, Chichester, 1983, 533 pp., *Surf. Interface Anal.* 6:302-302.  
488 <http://doi.org/10.1002/sia.740060611>

489 Chung C, Lee M, Choe EK (2004) Characterization of cotton fabric scouring by FT-IR ATR spectroscopy.  
490 *Carbohydr. Polym.* 58:417-420. <http://doi.org/10.1016/j.carbpol.2004.08.005>

491 Cools P, De Geyter N, Morent R (2015) Plasma modified textiles for biomedical applications. *Intech.*  
492 <http://doi.org/10.5772/59770>

493 De Geyter N, Sarani A, Jacobs T, Nikiforov AY, Desmet T, Dubruel P (2013) Surface Modification of Poly-  
494 epsilon-Caprolactone with an Atmospheric Pressure Plasma Jet. *Plasma Chem. Plasma Process.* 33:165-  
495 175. <http://doi.org/10.1007/s11090-012-9419-3>

496 Friedrich JF, Mix R, Schulze RD, Meyer-Plath A, Joshi R, Wettmarshausen S (2008) New plasma techniques for  
497 polymer surface modification with monotype functional groups. *Plasma Process. Polym.* 5:407-423.  
498 <https://doi.org/10.1002/ppap.200700145>

499 Garside P, Wyeth P (2003) Identification of cellulosic fibres by FTIR spectroscopy - Thread and single fibre  
500 analysis by attenuated total reflectance. *Stud. Conserv.* 48:269-275.  
501 <http://doi.org/10.1179/sic.2003.48.4.269>

502 Gorbanev Y, O'Connell D, Chechik V (2016) Non-Thermal Plasma in Contact with Water: The Origin of  
503 Species. *Chem. Eur. J.* 22:3496-3505. <https://doi.org/10.1002/chem.201503771>  
504

505 Gorjanc M, Bukošek V, Gorenšek M, Mozetič M (2010) CF<sub>4</sub> plasma and silver functionalized cotton. *Text. Res.*  
506 *J.* 80:2204-2213. <https://doi.org/10.1177/0040517510376268>

507 Haji A (2017) Improved natural dyeing of cotton by plasma treatment and chitosan coating; optimization by  
508 response surface methodology. *Cell. Chem. Technol.* 51:975-982.

509 Haji A (2019) Dyeing of Cotton Fabric with Natural Dyes Improved by Mordants and Plasma Treatment. *Prog.*  
510 *Color. Color. Coat.* 12:191-201.

511 Haji A, Barani H, Qavamnia SS (2013) In situ synthesis of silver nanoparticles onto cotton fibres modified with  
512 plasma treatment and acrylic acid grafting. *Micro Nano Lett.* 8:315-318.

513 Haji A, Qavamnia SS, Bizhaem FK (2016) Salt free neutral dyeing of cotton with anionic dyes using plasma and  
514 chitosan treatments. *Ind. Text.* 67:109-113

515 Holländer A, Wilken R, Behnisch J (1999) Subsurface chemistry in the plasma treatment of polymers. *Surf.*  
516 *Coat. Technol.* 116:788-791. [https://doi.org/10.1016/S0257-8972\(99\)00297-2](https://doi.org/10.1016/S0257-8972(99)00297-2)

517 Hsieh Y-L, Thompson J, Miller A (1996) Water wetting and retention of cotton assemblies as affected by  
518 alkaline and bleaching treatments. *Text. Res. J.* 66:456-464.  
519 <https://doi.org/10.1177/004051759606600707>

- 520 Ikawa S, Kitano K, Hamaguchi S (2010) Effects of pH on bacterial inactivation in aqueous solutions due to  
521 low-temperature atmospheric pressure plasma application. *Plasma Process. Polym.* 7:33-42.  
522 <https://doi.org/10.1002/ppap.200900090>
- 523 Ikegami T, Nakanishi F, Uchiyama M, Ebihara K (2004) Optical measurement in carbon nanotubes formation by  
524 pulsed laser ablation. *Thin Solid Films* 457:7-11. <http://doi.org/10.1016/j.tsf.2003.12.033>
- 525 Joshi R, Friedrich J, Krishna-Subramanian S (2013) Surface modification of ultra-high molecular weight  
526 polyethylene membranes using underwater plasma polymerization. *Plasma Chem. Plasma Process.*  
527 33:921-940. <http://doi.org/10.1007/s11090-013-9476-2>
- 528 Joshi R, Friedrich JF, Wagner M (2009a) Study of carboxylic functionalization of polypropylene surface using  
529 the underwater plasma technique. *Eur. Phys. J. D* 54:249-258. [http://doi.org/10.1140/epjd/e2009-00088-](http://doi.org/10.1140/epjd/e2009-00088-6)  
530 6
- 531 Joshi R, Schulze RD, Meyer-Plath A, Friedrich JF (2008) Selective surface modification of poly (propylene)  
532 with OH and COOH groups using liquid-plasma systems. *Plasma Process. Polym.* 5:695-707.  
533 <https://doi.org/10.1002/ppap.200700175>
- 534 Joshi R, Schulze RD, Meyer-Plath A, Wagner MH, Friedrich JF (2009b) Selective surface modification of  
535 polypropylene using underwater plasma technique or underwater capillary discharge. *Plasma Process. Polym.*  
536 6:S218-S222. <https://doi.org/10.1002/ppap.200930601>  
537
- 538 Jovančić P, Vilchez A, Molina R (2016) Synthesis of thermo-sensitive hydrogels from free radical  
539 copolymerization of NIPAAm with MBA initiated by atmospheric plasma treatment. *Plasma Process. Polym.*  
540 13:752-760. <https://doi.org/10.1002/ppap.201500194>  
541
- 542 Karahan H, Özdoğan E (2008) Improvements of surface functionality of cotton fibers by atmospheric plasma  
543 treatment. *Fiber. Polym.* 9:21-26.
- 544 Khlyustova A, Galmiz O, Zahoran M, Brablec A, Černak M (2015) Underwater discharge plasma-induced  
545 coating of poly (acrylic acid) on polypropylene fiber. *J. Mater. Sci.* 50:3504-3509.  
546 <http://doi.org/10.1007/s10853-015-8913-4>
- 547 Kolarova K, Vosmanska V, Rimpelova S, Svorcik V (2013) Effect of plasma treatment on cellulose fiber.  
548 *Cellulose* 20:953-961. <http://doi.org/10.1007/s10570-013-9863-0>
- 549 Liu DX, Bruggeman P, Iza F, Rong MZ, Kong MG (2010) Global model of low-temperature atmospheric-  
550 pressure He + H<sub>2</sub>O plasmas. *Plasma Sources Sci. Technol.* 19:025018. [https://doi.org/10.1088/0963-](https://doi.org/10.1088/0963-0252/19/2/025018)  
551 0252/19/2/025018
- 552 Liu H, Wang Y, Bowman JM (2016) Quantum Local Monomer IR Spectrum of Liquid D<sub>2</sub>O at 300 K from 0 to  
553 4000 cm<sup>-1</sup> Is in Near-Quantitative Agreement with Experiment. *J. Phys. Chem. B* 120:2824-2828.  
554 <https://doi.org/10.1021/acs.jpcc.6b01722>
- 555 Mihailović D et al. (2011) Functionalization of cotton fabrics with corona/air RF plasma and colloidal TiO<sub>2</sub>  
556 nanoparticles. *Cellulose* 18:811-825. <https://doi.org/10.1007/s10570-011-9510-6>
- 557 Molina R, Gómez M, Kan C-W, Bertran E (2014) Hydrophilic–oleophobic coatings on cellulosic materials by  
558 plasma assisted polymerization in liquid phase and fluorosurfactant complexation. *Cellulose* 21:729-  
559 739. <https://doi.org/10.1007/s10570-013-0131-0>
- 560 Molina R, Ligeró C, Jovančić P, Bertran E (2013a) In situ polymerization of aqueous solutions of NIPAAm  
561 initiated by atmospheric plasma treatment *Plasma Process. Polym.* 10:506-516.  
562 <https://doi.org/10.1002/ppap.201200121>  
563
- 564 Molina R, Sole I, Vilchez A, Bertran E, Solans C, Esquena J (2013b) Surface Functionalization of Macroporous  
565 Polymeric Materials by Treatment with Air Low Temperature. *Plasma J. Nanosci. Nanotechnol.*  
566 13:2819-2825 <https://doi.org/10.1166/jnn.2013.7369>

- 567 Molina R, Teixidó JM, Kan C-W, Jovančić P (2017a) Hydrophobic coatings on cotton obtained by in situ plasma  
568 polymerization of a fluorinated monomer in ethanol solutions. *ACS Appl. Mater. Interfaces* 9:5513-  
569 5521. <https://doi.org/10.1021/acsami.6b15812>
- 570 Molina R, Teixidó JM, Kan C-W, Jovančić P (2017b) Hydrophobic coatings on cotton obtained by in situ plasma  
571 polymerization of a fluorinated monomer in ethanol solutions. *ACS Appl. Mater. Interfaces* 9:5513-  
572 5521. <https://doi.org/10.1021/acsami.6b15812>
- 573 Morent R, De Geyter N, Leys C, Gengembre L, Payen E (2008) Comparison between XPS- and FTIR-analysis  
574 of plasma-treated polypropylene film surfaces. *Surf. Interface Anal.* 40:597-600  
575 <https://doi.org/10.1002/Sia.2619>
- 576 Patino A, Canal C, Rodríguez C, Caballero G, Navarro A, Canal JM (2011) Surface and bulk cotton fibre  
577 modifications: plasma and cationization. Influence on dyeing with reactive dye. *Cellulose* 18:1073-  
578 1083. <https://doi.org/10.1007/s10570-011-9554-7>
- 579 Rajasekaran P, Muthuraman B (2019) Effect of Plasma Pre-treatment on the Conductivity of Polypyrrole-coated  
580 Cotton Fabric. *Fiber. Polym.* 20:2114-2119. <https://doi.org/10.1007/s12221-019-1177-x>
- 581 Sun D, Stylios G (2004) Effect of low temperature plasma treatment on the scouring and dyeing of natural  
582 fabrics. *Text. Res. J.* 74:751-756. <https://doi.org/10.1177/004051750407400901>
- 583 Tani A, Ono Y, Fukui S, Ikawa S, Kitano K (2012) Free radicals induced in aqueous solution by non-contact  
584 atmospheric-pressure cold plasma. *Appl. Phys. Lett.* 100:254103. <https://doi.org/10.1063/1.4729889>
- 585 Tatoulian M, Arefi-Khonsari F, Mabillet-Rouger I, Amouroux J, Gheorgiu M, Bouchier D (1995) Role of helium  
586 plasma pretreatment in the stability of the wettability, adhesion, and mechanical properties of ammonia plasma-  
587 treated polymers. Application to the Al-polypropylene system. *J. Adhes. Sci. Technol.* 9:923-934.  
588 <https://doi.org/10.1163/156856195X00798>
- 589 Topalovic T, Nierstrasz VA, Bautista L, Jovic D, Navarro A, Warmoeskerken M (2007) Analysis of the effects  
590 of catalytic bleaching on cotton. *Cellulose* 14:385-400. <https://doi.org/10.1007/s10570-007-9120-5>
- 591 Van Deynse A, De Geyter N, Leys C, Morent R (2014) Influence of water vapor addition on the surface  
592 modification of polyethylene in an argon dielectric barrier discharge. *Plasma Process. Polym.* 11:117-125.  
593 <https://doi.org/10.1002/ppap.201300088>
- 594 Van Deynse A, Morent R, Leys C, De Geyter N (2017) Influence of ethanol vapor addition on the surface  
595 modification of polyethylene in a dielectric barrier discharge. *Appl. Surf. Sci.* 419:847-859.  
596 <https://doi.org/10.1016/j.apsusc.2017.05.111>
- 597 Wang C, Liu Y, Xu H, Ren Y, Qiu Y (2008) Influence of atmospheric pressure plasma treatment time on  
598 penetration depth of surface modification into fabric. *Appl. Surf. Sci.* 254:2499-2505.  
599 <https://doi.org/10.1016/j.apsusc.2007.09.074>
- 600 Wang X et al. (2019) The Application of Atmospheric Plasma for Cotton Fabric Desizing. *Fiber. Polym.*  
601 20:2334-2341. <https://doi.org/10.1007/s12221-019-9330-0>
- 602 Yanguas-Gil A, Hueso JL, Cotrino J, Caballero A, Gonzalez-Elipe AR (2004) Reforming of ethanol in a  
603 microwave surface-wave plasma discharge. *Appl. Phys. Lett.* 85:4004-4006.  
604 <https://doi.org/10.1063/1.1808875>
- 605 Yasuda H, Hirotsu T (1978) Critical evaluation of conditions of plasma polymerization. *J. Polym. Sci. Pol.*  
606 *Chem.* 16:743-759. <https://doi.org/10.1002/pol.1978.170160403>  
607

## 608 **List of Figure Legends**

609 **Fig.1** Experimental atmospheric plasma set-up scheme

610 **Fig.2** UV-VIS emission spectra obtained during the He plasma treatment of cotton and cotton impregnated with  
611 different liquids (H<sub>2</sub>O, D<sub>2</sub>O and EtOH) at 30 (a) and 300 s (b)

612 **Fig.3** ATR-FTIR spectra obtained on non-impregnated (a) and H<sub>2</sub>O (b), D<sub>2</sub>O (c) and EtOH (d) impregnated  
613 cotton samples after 1, 3 and 6 cycles of consecutive impregnation/300 s He plasma treatment. UT stands for the  
614 untreated cotton sample. Enlarged carboxylate region (1800-1500 cm<sup>-1</sup>) obtained for cotton samples impregnated  
615 with H<sub>2</sub>O (e) and EtOH (f)

616 **Fig.4** XPS high-resolution C1s spectra of untreated cotton, cotton treated with He plasma and cotton  
617 impregnated with different liquids and subsequently treated by He plasma

618 **Fig.5** SEM images of cotton treated with He plasma and cotton impregnated with different liquids and  
619 subsequently treated by He plasma

620

## 621 **List of Table Titles**

622 Table 1. Elemental composition (%) at the surface determined by XPS on cotton treated by He plasma and cotton  
623 impregnated with different liquids and subsequently treated by He plasma (300 s).

624 Table 2. Relative concentrations of carbon bonds on untreated cotton, cotton treated with He plasma and cotton  
625 impregnated with different liquids and subsequently treated by He plasma.